2013

Scalar Differential Equation for Slowly-Varying Thickness-Shear Modes in AT-Cut Quartz Resonators With Surface Impedance for Acoustic Wave Sensor Application

Huijing He
University of Nebraska-Lincoln, he.hui.jing@hotmail.com

Jiashi Yang
University of Nebraska-Lincoln, jyang1@unl.edu

John A. Kosinski
Advanced Technology Group, MacAulay-Brown Inc., Dayton, OH, j.a.kosinski@ieee.org

Pages: 4349 - 4355, DOI: 10.1109/JSEN.2013.2267540

Scalar Differential Equation for Slowly-Varying Thickness-Shear Modes in AT-Cut Quartz Resonators With Surface Impedance for Acoustic Wave Sensor Application

Huijing He, Jiashi Yang, *Senior Member, IEEE*, and John A. Kosinski, *Fellow, IEEE*

***Abstract*— For time-harmonic motions, we generalize a 2-D scalar differential equation derived previously by Tiersten for slowly-varying thickness-shear vibrations of AT-cut quartz resonators. The purpose of the generalization is to include the effects of surface acoustic impedance from, e.g., mass layers or fluids for sensor applications. In addition to the variation of fields along the plate thickness, which is considered in the usual 1-D acoustic wave sensor models, the equation obtained also describes in-plane variations of the fields, and therefore can be used to study the vibrations of finite plate sensors with edge effects. The equation is compared with the theory of piezoelectricity in the special cases of acoustic waves and pure thickness vibrations in unbounded plates. An example of a finite rectangular plate is also given.**

***Index Terms*— Quartz, plate, resonator, sensor.**

I. Introduction

RESONANT frequencies of an elastic body can be affected by many effects, e.g., a temperature change, initial stress, surface mass layers, contact with a fluid, etc. Therefore, detection of frequency shifts in a vibrating body (resonator) can be used as the basis for making various acoustic wave sensors. Specifically, when a thin layer of another material is added to the surface of a quartz resonator, its resonant frequencies become lower due to the inertia of the mass layer [1]–[7]. This phenomenon has been used to make sensors for measuring the density and/or thickness of a mass layer. Such sensors are called quartz crystal microbalances (QCMs) and have applications in monitoring thin film deposition and in chemical and biological sensing [8]. Most QCMs are made from AT-cut quartz plates operating with thickness-shear (TSh) modes [9]–[11]. The mass sensitivity of QCMs is given by the well-known Sauerbrey equation [1].

Both particle displacements and the electric potential of pure TSh modes have spatial variations along the plate thickness direction only. Such modes can only exist in unbounded plates carrying unbounded and uniform mass layers. These modes can be analyzed using various one-dimensional models [12]–[21]. The operating modes in real devices have in-plane variations due to edge effects of finite plates. Clearly, one-dimensional models cannot describe these in-plane variations. The in-plane variation causes a deviation from the sensitivity as calculated using the Sauerbrey equation [22]. In a typical QCM, the mass layer covers the central portion of the crystal plate only. The vibration is largely confined under the mass layer and decays rapidly outside it. This phenomenon is another important aspect of the in-plane variation of modes and is referred to as energy trapping [23]. Energy trapping is crucial in the design of device mounting structures in that losses are minimized by mounting at points near the plate edges where there is little vibration. In-plane mode variation is also important in the design of monolithic arrays of QCMs where sufficient energy trapping is necessary to avoid undesirable interactions among neighboring QCMs [24]–[26]. Theoretical studies of in-plane variations of modes in QCMs on finite plates are relatively few [27]–[31] because of the mathematical complications arising from material anisotropy and electromechanical coupling.

Tiersten once derived a two-dimensional scalar differential equation for TSh modes in AT-cut quartz resonators with slow in-plane variations [32]–[35]. The equation is simple and accurate, and has been widely used in analyzing finite quartz resonators [36]–[41]. However, in the derivation of the scalar equation, the quartz plate surfaces are taken either as free or as carrying thin electrodes only. Therefore, Tiersten's equation cannot be used to analyze QCMs with additional surface mass layers or with fluid on the surface. In this paper we generalize Tiersten's equation to include the effects of surface acoustic impedance in a general manner, which then includes mass layers or fluids as special cases. The equation obtained can be used to analyze finite QCMs.

II. Unelectroded Plates

Consider an AT-cut quartz plate as shown in Fig. 1. The plate thickness is $2h$ which is much smaller than the length $2a$ and width $2c$. x_2 is normal to the plate. x_1 and x_3 are in the middle plane of the plate. Unelectroded and electroded plates need to be treated separately and we consider unelectroded plates first.

Manuscript received April 18, 2013; revised May 30, 2013; accepted June 6, 2013. Date of publication June 10, 2013; date of current version September 27, 2013. This work was supported in part by the U.S. Army Research Laboratory/U.S. Army Research Office under Grant W911NF-10-1-0293. The associate editor coordinating the review of this paper and approving it for publication was Dr. Stefan J. Rupitsch.

H. He and J. Yang are with the Department of Mechanical and Materials Engineering, University of Nebraska-Lincoln, Lincoln, NE 68588-0526 USA (e-mail: he.hui.jing@hotmail.com; jyang1@unl.edu).

J. A. Kosinski is with Advanced Technology Group, MacAulay-Brown Inc., Dayton, OH 45430 USA (e-mail: j.a.kosinski@ieee.org).

Digital Object Identifier 10.1109/JSEN.2013.2267540

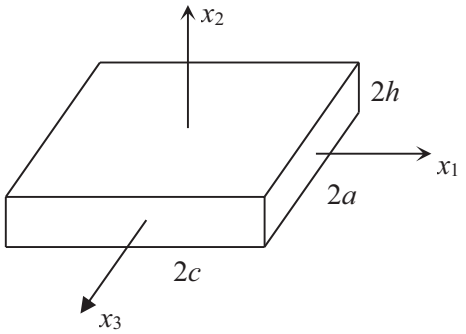

Fig. 1. An AT-cut quartz plate and coordinate system.

Let the elastic, piezoelectric, and dielectric constants be c_{pq}, e_{ip}, and ε_{ij} according to the Voigt notation. As in [32], we neglect the relatively small elastic constants c_{14}, c_{24} and c_{56}. We also neglect the x_1 and x_3 dependence of the electric potential ϕ for this case of small piezoelectric coupling [32]. These approximations decouple the displacement component u_3 from u_1 and u_2. We are concerned with coupled motions of u_1 and u_2 which are governed by [32]:

$$\begin{aligned} &c_{11}u_{1,11} + (c_{12}+c_{66})u_{2,12} + c_{66}u_{1,22} \\ &\qquad + c_{55}u_{1,33} + e_{26}\phi_{,22} = \rho\ddot{u}_1, \\ &c_{66}u_{2,11} + (c_{12}+c_{66})u_{1,12} + c_{22}u_{2,22} = \rho\ddot{u}_2, \\ &e_{26}u_{1,22} - \varepsilon_{22}\phi_{,22} = 0, \end{aligned} \tag{1}$$

where a comma followed by an index denotes partial differentiation. A superimposed dot represents a time derivative. Constitutive equations relevant to the boundary conditions at the plate top and bottom are [32]:

$$\begin{aligned} T_{22} &= c_{12}u_{1,1} + c_{22}u_{2,2}, \\ T_{12} &= c_{66}(u_{1,2} + u_{2,1}) + e_{26}\phi_{,2}, \\ D_2 &= e_{26}u_{1,2} - \varepsilon_{22}\phi_{,2}, \end{aligned} \tag{2}$$

where T_{ij} and D_i are the stress and electric displacement components. The boundary conditions at $x_2 = \pm h$ are

$$\begin{aligned} &T_{22} = -Z_n\dot{u}_2, \quad T_{21} = -Z_t\dot{u}_1, \quad D_2 = 0, \quad x_2 = h, \\ &T_{22} = Z_n\dot{u}_2, \quad T_{21} = Z_t\dot{u}_1, \quad D_2 = 0, \quad x_2 = -h, \end{aligned} \tag{3}$$

where Z_n and Z_t are the normal and tangential acoustic impedances on the surfaces of the plate [42]–[44]. We consider the case of what may be called "isotropic" acoustic impedance, i.e., the impedances in the tangential and normal directions are not coupled. This allows for the existence of the u_1 dominated TSh modes for AT-cut quartz. In more general situations the impedances can be represented by a 3 × 3 matrix [42], [43] which may possess couplings among displacement components in different directions. The impedances are frequency dependent in general.

We select ϕ as [32]

$$\phi = (e_{26}/\varepsilon_{22})u_1. \tag{4}$$

$(1)_3$ and $D_2 = 0$ are thus satisfied. Substituting (4) into $(1)_{1,2}$ and $(2)_{1,2}$, we obtain:

$$\begin{aligned} &c_{11}u_{1,11} + (c_{12}+c_{66})\,u_{2,12} + \bar{c}_{66}u_{1,22} + c_{55}u_{1,33} = \rho\ddot{u}_1, \\ &c_{66}u_{2,11} + (c_{12}+c_{66})\,u_{1,12} + c_{22}u_{2,22} = \rho\ddot{u}_2, \end{aligned} \tag{5}$$

$$T_{22} = c_{12}u_{1,1} + c_{22}u_{2,2}, \quad T_{12} = \bar{c}_{66}u_{1,2} + c_{66}u_{2,1}, \tag{6}$$

where $\bar{c}_{66} = c_{66} + e_{26}^2/\varepsilon_{22}$. We look for solutions to (5) in the following form:

$$\begin{aligned} u_1 &= B_1 \sin(\eta\, x_2)\exp(-\xi\, x_1)\cos(\nu\, x_3)\exp(i\omega t), \\ u_2 &= B_2 \cos(\eta\, x_2)\exp(-\xi\, x_1)\cos(\nu\, x_3)\exp(i\omega t), \end{aligned} \tag{7}$$

where B_1 and B_2 are undetermined constants, ω is the frequency of the vibration, and η is the wave number along the plate thickness. ξ and ν are the in-plane wave numbers which are small for long or slowly varying modes. Substitution of (7) into (5) leads to

$$\begin{aligned} &\left(\rho\omega^2 + c_{11}\xi^2 - \bar{c}_{66}\eta^2 - c_{55}\nu^2\right)B_1 + (c_{12}+c_{66})\,\xi\eta B_2 = 0, \\ &-(c_{12}+c_{66})\,\xi\eta B_1 + \left(\rho\omega^2 + c_{66}\xi^2 - c_{22}\eta^2\right)B_2 = 0. \end{aligned} \tag{8}$$

For nontrivial solutions, the determinant of the coefficient matrix of (8) must vanish. To the zeroth order in ξ and ν, we have

$$\eta_1^2 = \rho\omega^2/\bar{c}_{66}, \quad \eta_2^2 = \rho\omega^2/c_{22}. \tag{9}$$

To the second order in ξ and ν, we have

$$B_2^{(1)} = \frac{r\xi}{\eta_1}B_1^{(1)}, \quad B_1^{(2)} = \frac{r\xi}{\eta_2}B_2^{(2)}, \tag{10}$$

$$r = (c_{12}+c_{66})/(\bar{c}_{66} - c_{22}). \tag{11}$$

From (9) we also have

$$\eta_2 = \kappa\eta_1, \quad \kappa = \sqrt{\bar{c}_{66}/c_{22}}. \tag{12}$$

In order to satisfy the boundary conditions in (3), we take a sum of the two asymptotic solutions of (8) [33]:

$$\begin{aligned} u_1 &= \left[B_1^{(1)}\sin(\eta_1 x_2) + B_1^{(2)}\sin(\eta_2 x_2)\right] \\ &\quad \times \exp(-\xi x_1)\cos(\nu x_3)\exp(i\omega t), \\ u_2 &= \left[B_2^{(1)}\cos(\eta_1 x_2) + B_2^{(2)}\cos(\eta_2 x_2)\right] \\ &\quad \times \exp(-\xi x_1)\cos(\nu x_3)\exp(i\omega t). \end{aligned} \tag{13}$$

Substituting (13) into (3) with (6), and using (10), we obtain

$$\begin{aligned} &B_1^{(1)}\left(\bar{c}_{66}\eta_1 - c_{66}r\frac{\xi^2}{\eta_1}\right)\cos(\eta_1 h) \\ &+B_2^{(2)}\xi\,(r\bar{c}_{66} - c_{66})\cos(\eta_2 h) \\ &\quad = -Z_t(\omega)(i\omega)\left[\sin(\eta_1 h)\,B_1^{(1)} + \frac{r\xi}{\eta_2}\sin(\eta_2 h)\,B_2^{(2)}\right], \\ &B_1^{(1)}\xi\,(c_{12} + c_{22}r)\sin(\eta_1 h) \\ &+B_2^{(2)}\left(c_{22}\eta_2 + c_{12}r\frac{\xi^2}{\eta_2}\right)\sin(\eta_2 h) \\ &\quad = -Z_n(\omega)(i\omega)\left[\frac{r\xi}{\eta_1}\cos(\eta_1 h)\,B_1^{(1)} + \cos(\eta_2 h)\,B_2^{(2)}\right]. \end{aligned} \tag{14}$$

We are interested in vibrations near in frequency to the odd pure TSh mode whose $\eta_1 h = n\pi/2$. Therefore we write

$$\eta_1 h = n\pi/2 + \alpha_n, \quad n = 1, 3, 5\ldots, \tag{15}$$

where α_n is small. Substituting (15) into (14), expanding the resulting trigonometric functions in powers of α_n, and retaining terms linear in α_n, we arrive at

$$\begin{aligned}
&B_1^{(1)}\left(\bar{c}_{66}\eta_1 - c_{66}r\frac{\xi^2}{\eta_1}\right)(-1)^{\frac{n+1}{2}}\alpha_n \\
&+B_2^{(2)}\xi\left(r\bar{c}_{66}-c_{66}\right)\cos\left(\eta_2 h\right) \\
&\quad = -Z_t\left(\omega\right)\left(i\omega\right)\left[(-1)^{\frac{n-1}{2}}B_1^{(1)} + \frac{r\xi}{\eta_2}\sin\left(\eta_2 h\right)B_2^{(2)}\right], \\
&B_1^{(1)}\xi\left(c_{12}+c_{22}r\right)(-1)^{\frac{n-1}{2}} \\
&+B_2^{(2)}\left(c_{22}\eta_2 + c_{12}r\frac{\xi^2}{\eta_2}\right)\sin\left(\eta_2 h\right) \\
&\quad = -Z_n\left(\omega\right)\left(i\omega\right)\left[\frac{r\xi}{\eta_1}(-1)^{\frac{n+1}{2}}\alpha_n B_1^{(1)} + \cos\left(\eta_2 h\right)B_2^{(2)}\right].
\end{aligned} \tag{16}$$

(16) is a system of linear homogeneous equations in $B_1^{(1)}$ and $B_2^{(2)}$. For nontrivial solutions the determinant of its coefficient matrix has to vanish, which leads to an equation for α_n. For long waves and small acoustic impedance,

$$\begin{aligned}
\alpha_n = &\frac{4h^2\left(c_{12}+c_{22}r\right)\left(r\bar{c}_{66}-c_{66}\right)\cot\left(\kappa n\pi/2\right)}{\bar{c}_{66}c_{22}\kappa\left(n\pi\right)^2}\xi^2 \\
&+\frac{i\omega}{\bar{c}_{66}\eta_1}Z_t\left(\omega\right).
\end{aligned} \tag{17}$$

We note that (17) does not have Z_n. This is not surprising because for the thickness-shear mode we are considering the normal impedance should be a higher-order effect. Substituting (10), (15), and (17) into $(8)_1$, and retaining terms linear in α_n, we obtain an approximate dispersion relation accurate to the second order of the small in-plane wave numbers ξ and ν:

$$M_n\xi^2 - c_{55}\nu^2 - \bar{c}_{66}\left(\frac{n\pi}{2h}\right)^2 - \frac{2i\omega}{h}Z_t\left(\omega\right) + \rho\omega^2 = 0, \tag{18}$$

$$\begin{aligned}
M_n = &\, c_{11} + \left(c_{12}+c_{66}\right)r + 4\left(c_{12}+c_{22}r\right)\left(r\bar{c}_{66}-c_{66}\right) \\
&\times\cot\left(\kappa n\pi/2\right)/\left(c_{22}\kappa n\pi\right).
\end{aligned} \tag{19}$$

From (18), we can construct the following two-dimensional scalar differential equation whose dispersion relation is (18):

$$\begin{aligned}
M_n\frac{\partial^2 u_1^n}{\partial x_1^2} + c_{55}\frac{\partial^2 u_1^n}{\partial x_3^2} - \bar{c}_{66}\left(\frac{n\pi}{2h}\right)^2 u_1^n \\
+\left[\rho\omega^2 - \left(2i\omega/h\right)Z_t\left(\omega\right)\right]u_1^n = 0,
\end{aligned} \tag{20}$$

where the subscript "n" denotes the nth antisymmetric essentially TSh mode, i.e., $u_1 = \Sigma u_1^n(x_1,x_3)\sin(\eta_1^n x_2)$, $n = 1,3,5,\ldots$. When the acoustic impedance $Z_t$in (20) is set to zero, (20) reduces to (1) of [35].

III. Electroded Plates

For electroded plates, we consider free vibrations first and then extend the results to electrically forced vibrations.

A. Free Vibration

For plates with identical and thin electrodes at the top and bottom, let the electrode thickness be $2h'$and let the electrode density be ρ'. In this case (1) and (2) still apply. (3) becomes:

$$\begin{aligned}
&T_{22} = -2\rho' h'\ddot{u}_2 - Z_n\dot{u}_2, \quad T_{21} = -2\rho' h'\ddot{u}_1 - Z_t\dot{u}_1, \\
&\phi = 0, \quad x_2 = h, \\
&T_{22} = 2\rho' h'\ddot{u}_2 + Z_n\dot{u}_2, \quad T_{21} = 2\rho' h'\ddot{u}_1 + Z_t\dot{u}_1, \\
&\phi = 0, \quad x_2 = -h.
\end{aligned} \tag{21}$$

We select ϕ as [32]

$$\phi = e_{26}u_1/\varepsilon_{22} - e_{26}u_1\left(h\right)x_2/(\varepsilon_{22}h). \tag{22}$$

ϕ satisfies $(1)_3$ and the electrical boundary conditions. Substitution of ϕ into $(1)_{1,2}$ and $(2)_{1,2}$ still leads to (5), but (6) becomes

$$\begin{aligned}
T_{22} &= c_{12}u_{1,1} + c_{22}u_{2,2}, \\
T_{12} &= \bar{c}_{66}u_{1,2} + c_{66}u_{2,1} - e_{26}^2 u_1\left(h\right)/(\varepsilon_{22}h).
\end{aligned} \tag{23}$$

We seek an approximate solution to (5) in the form:

$$\begin{aligned}
u_1 &= B_1\sin(\eta x_2)\cos(\xi x_1)\cos(\nu x_3)\exp(i\omega t), \\
u_2 &= B_2\cos(\eta x_2)\sin(\xi x_1)\cos(\nu x_3)\exp(i\omega t).
\end{aligned} \tag{24}$$

Substitution of (24) into (5) gives

$$\begin{aligned}
&\left(c_{11}\xi^2 + \bar{c}_{66}\eta^2 + c_{55}\nu^2 - \rho\omega^2\right)B_1 + \left(c_{12}+c_{66}\right)\xi\eta B_2 = 0, \\
&\left(c_{12}+c_{66}\right)\xi\eta B_1 + \left(c_{66}\xi^2 + c_{22}\eta^2 - \rho\omega^2\right)B_2 = 0.
\end{aligned} \tag{25}$$

To zero order in ξ and ν, we still have (9). To the second order in $\xi$and ν, we still have (10). (11) and (12) also remain the same.

In order to satisfy (21), we take [33]:

$$\begin{aligned}
u_1 &= \left\{B_1^{(1)}\sin\left(\eta_1 x_2\right) + B_1^{(2)}\sin\left(\eta_2 x_2\right)\right\}\cos\left(\xi x_1\right)\cos\left(\nu x_3\right), \\
u_2 &= \left\{B_2^{(1)}\cos\left(\eta_1 x_2\right) + B_2^{(2)}\cos\left(\eta_2 x_2\right)\right\}\sin\left(\xi x_1\right)\cos\left(\nu x_3\right),
\end{aligned} \tag{26}$$

where the $\exp(i\omega t)$ factor has been omitted for convenience. Substituting (26) into (21) with (23), and simplifying it by (10), we obtain

$$\begin{aligned}
&B_1^{(1)}\left[\left(\bar{c}_{66}\eta_1 + c_{66}r\frac{\xi^2}{\eta_1}\right)\cos\left(\eta_1 h\right)\right. \\
&\qquad\left. -\left(e_{26}^2/(\varepsilon_{22}h) + 2\rho' h'\omega^2 - Z_t\left(\omega\right)i\omega\right)\sin\left(\eta_1 h\right)\right] \\
&+B_2^{(2)}\left[\xi\left(c_{66}-r\bar{c}_{66}\right)\cos\left(\eta_2 h\right) + \frac{\xi r}{\eta_2}\right. \\
&\qquad\left.\times\left(e_{26}^2/(\varepsilon_{22}h) + 2\rho' h'\omega^2 - Z_t\left(\omega\right)i\omega\right)\sin\left(\eta_2 h\right)\right] = 0, \\
&B_1^{(1)}\left[\xi\left(c_{12}+c_{22}r\right)\sin\left(\eta_1 h\right)\right. \\
&\qquad\left. +\left(2\rho' h'\omega^2 - Z_n\left(\omega\right)i\omega\right)\frac{r\xi}{\eta_1}\cos\left(\eta_1 h\right)\right] \\
&+B_2^{(2)}\left[\left(c_{22}\eta_2 - c_{12}r\frac{\xi^2}{\eta_2}\right)\sin\left(\eta_2 h\right)\right. \\
&\qquad\left. +\left(2\rho' h'\omega^2 - Z_n\left(\omega\right)i\omega\right)\cos(\eta_2 h)\right] = 0.
\end{aligned} \tag{27}$$

We are interested in vibrations near the pure TSh modes. Let

$$\eta_1 h = n\pi/2 + \beta_n, \quad n = 1, 3, 5 \cdots, \tag{28}$$

where β_n is small. Substituting (28) into (27), expanding the resulting trigonometric functions in powers of β_n, and retaining terms linear in β_n, we have

$$\begin{aligned}
&B_1^{(1)}\left[\left(\bar{c}_{66}\eta_1 + c_{66}r\frac{\xi^2}{\eta_1}\right)(-1)^{\frac{n+1}{2}}\beta_n - L(-1)^{\frac{n-1}{2}}\right] \\
&\quad + B_2^{(2)}\xi\left[(c_{66} - r\bar{c}_{66})\cos(\eta_2 h) + \frac{r}{\eta_2}L\sin(\eta_2 h)\right] = 0 \\
&B_1^{(1)}\xi\left[(c_{12} + c_{22}r)(-1)^{\frac{n-1}{2}}\right. \\
&\quad \left. + \left(Rh\bar{c}_{66}\eta_1 r - Z_n(\omega)\, i\omega\frac{r\xi}{\eta_1}\right)(-1)^{\frac{n+1}{2}}\beta_n\right] \\
&+ B_2^{(2)}\left[\left(c_{22}\eta_2 - c_{12}r\frac{\xi^2}{\eta_2}\right)\sin(\eta_2 h)\right. \\
&\quad \left. + \left(Rh\bar{c}_{66}\eta_1^2 - Z_n(\omega)\, i\omega\right)\cos(\eta_2 h)\right] = 0,
\end{aligned} \tag{29}$$

where

$$\begin{aligned}
L &= \bar{c}_{66}\left(k_{26}^2 + R\eta_1^2 h^2\right)/h - Z_t(\omega)\, i\omega, \\
k_{26} &= \sqrt{e_{26}^2/(\bar{c}_{66}\varepsilon_{22})}, \quad R = 2\rho' h'/(\rho h).
\end{aligned} \tag{30}$$

(29) is a system of linear homogeneous equations in $B_1^{(1)}$ and $B_2^{(2)}$. For nontrivial solutions, the determinant of the coefficient matrix must vanish which determines

$$\begin{aligned}
\beta_n = &\frac{4h^2(c_{12} + c_{22}r)(r\bar{c}_{66} - c_{66})\cot(\kappa n\pi/2)}{\bar{c}_{66}c_{22}\kappa(n\pi)^2}\xi^2 \\
&- \frac{2k_{26}^2}{n\pi} - \frac{n\pi}{2}R + \frac{2Z_t(\omega)\, i\omega h}{\bar{c}_{66}n\pi}.
\end{aligned} \tag{31}$$

Substituting (10), (28) and (31) into $(25)_1$ and retaining terms linear in β_n, we obtain

$$M_n\xi^2 + c_{55}\nu^2 + \hat{c}_{66}\left(\frac{n\pi}{2h}\right)^2 - \rho\omega^2 + \frac{2}{h}i\omega Z_t(\omega) = 0, \tag{32}$$

$$\hat{c}_{66} = \bar{c}_{66}\left(1 - 2R - 8k_{26}^2/(n^2\pi^2)\right). \tag{33}$$

M_n is still given by (19). From (32), we construct the following scalar equation whose dispersion relation is (32):

$$\begin{aligned}
&M_n\frac{\partial^2 u_1^n}{\partial x_1^2} + c_{55}\frac{\partial^2 u_1^n}{\partial x_3^2} - \hat{c}_{66}\left(\frac{n\pi}{2h}\right)^2 u_1^n \\
&\quad + \rho\omega^2 u_1^n - \frac{2}{h}i\omega Z_t(\omega)\, u_1^n = 0.
\end{aligned} \tag{34}$$

When $Z_t = 0$, (34) reduces to the homogeneous part of (2.14) in [34].

B. Electrically Forced Vibration

Consider the case when there is an applied voltage $2V\exp(i\omega t)$ across the electrodes. In this case (1) and (2) still apply. (3) becomes:

$$\begin{aligned}
T_{22} &= -2\rho' h'\ddot{u}_2 - Z_n\dot{u}_2, \quad T_{21} = -2\rho' h'\ddot{u}_1 - Z_t\dot{u}_1, \\
\phi &= V\exp(i\omega t), \quad x_2 = h, \\
T_{22} &= 2\rho' h'\ddot{u}_2 + Z_n\dot{u}_2, \quad T_{21} = 2\rho' h'\ddot{u}_1 + Z_t\dot{u}_1, \\
\phi &= -V\exp(i\omega t), \quad x_2 = -h.
\end{aligned} \tag{35}$$

We make the following change of dependent variables [34]:

$$\begin{aligned}
u_1 &= \tilde{u}_1 + Kx_2, \quad u_2 = \tilde{u}_2, \\
\phi &= \frac{x_2}{h}V + \frac{e_{26}}{\varepsilon_{22}}\tilde{u}_1 - \frac{e_{26}}{\varepsilon_{22}}\frac{x_2}{h}\tilde{u}_1(h),
\end{aligned} \tag{36}$$

where $K = -e_{26}V/(c_{66}h)$ [34]. (36) transforms $(1)_{1,2}$ and the mechanical boundary conditions in (35) into:

$$\begin{aligned}
&c_{11}\tilde{u}_{1,11} + (c_{12} + c_{66})\tilde{u}_{2,12} + \bar{c}_{66}\tilde{u}_{1,22} + c_{55}\tilde{u}_{1,33} \\
&\quad = -\rho\omega^2\tilde{u}_1 - \rho\omega^2 Kx_2, \\
&c_{66}\tilde{u}_{2,11} + (c_{12} + c_{66})\tilde{u}_{1,12} + c_{22}\tilde{u}_{2,22} = -\rho\omega^2\tilde{u}_2,
\end{aligned} \tag{37}$$

$$\begin{aligned}
&c_{66}\tilde{u}_{2,1} + \bar{c}_{66}\tilde{u}_{1,2} - e_{26}^2\tilde{u}_1(h)/(\varepsilon_{22}h) \\
&\quad = \pm 2\rho' h'\omega^2\tilde{u}_1 \mp i\omega Z_t\tilde{u}_1 + 2\rho' h'\omega^2 Kh, \ \ x_2 = \pm h, \\
&c_{22}\tilde{u}_{2,2} + c_{12}\tilde{u}_{1,1} = \pm 2\rho' h'\omega^2\tilde{u}_2 \mp i\omega Z_n\tilde{u}_2, \ \ x_2 = \pm h.
\end{aligned} \tag{38}$$

$(1)_3$ and the electrical boundary conditions in (35) are satisfied. We write the solution to (37) and (38) as a series using the asymptotic eigensolutions of their homogeneous form (now denoted by $\tilde{u}_1^n$) as basis functions, i.e.,

$$\tilde{u}_1 = \sum_{n=1,3,5}^{\infty}\tilde{u}_1^n\sin(\eta_1^n x_2), \tag{39}$$

where, in the forced vibration only, the relatively small $\tilde{u}_2$ has been taken as approximately zero [33]. Furthermore, in $\tilde{u}_1^n$, the $B_1^{(2)}$ part is much smaller than the $B_1^{(1)}$ part and can be neglected [33]. Therefore,

$$\tilde{u}_1^n \cong B_1^{(1)n}\cos(\xi x_1)\cos(\nu x_3). \tag{40}$$

From $(37)_1$, to the second order in ξ and ν, the governing equation for the inhomogeneous solution can be written in the following form:

$$\begin{aligned}
\sum_{n=1,3,5}^{\infty}&\left[M_n\frac{\partial^2\tilde{u}_1^n}{\partial x_1^2} + c_{55}\frac{\partial^2\tilde{u}_1^n}{\partial x_3^2} - \hat{c}_{66}\left(\frac{n\pi}{2h}\right)^2\tilde{u}_1^n + \rho\omega^2\tilde{u}_1^n\right. \\
&\left. - \frac{2}{h}i\omega Z_t(\omega)\,\tilde{u}_1^n\right]\sin(\eta_1^n x_2) = \rho\omega^2\frac{e_{26}Vx_2}{c_{66}h}\exp(i\omega t).
\end{aligned} \tag{41}$$

Then, utilizing the orthogonality of $\sin(\eta_1^n x_2)$ over the interval $(-h, h)$, from (41) we obtain the following equation for $\tilde{u}_1^n$:

$$\begin{aligned}
&M_n\frac{\partial^2\tilde{u}_1^n}{\partial x_1^2} + c_{55}\frac{\partial^2\tilde{u}_1^n}{\partial x_3^2} - \hat{c}_{66}\left(\frac{n\pi}{2h}\right)^2\tilde{u}_1^n + \rho\omega^2\tilde{u}_1^n - \frac{2i\omega}{h}Z_t(\omega)\tilde{u}_1^n \\
&\quad = (-1)^{\frac{n-1}{2}}\rho\omega^2\frac{e_{26}}{c_{66}}\frac{8V(1+R)}{n^2\pi^2}.
\end{aligned} \tag{42}$$

With $\tilde{u}_1$determined through $\tilde{u}_1^n$ governed by (42), to further determine $u_1 = \Sigma u_1^n\sin(\eta_1^n x_2)$, we need to expand the inhomogeneous term in $(36)_1$ as:

$$Kx_2 = \sum_{n=1,3,5}^{\infty}A_n\sin\left(\eta_1^n x_2\right)\cos(\xi x_1)\cos(\nu x_3), \tag{43}$$

where

$$A_n = -(-1)^{\frac{n-1}{2}}\rho\frac{e_{26}}{c_{66}}\frac{8V(1+R)}{n^2\pi^2}. \tag{44}$$

Then (42) can be converted to an equation for u_1^n [11]:

$$M_n \frac{\partial^2 u_1^n}{\partial x_1^2} + c_{55} \frac{\partial^2 u_1^n}{\partial x_3^2} - \hat{c}_{66} \left(\frac{n\pi}{2h}\right)^2 u_1^n + \rho\omega^2 u_1^n - \frac{2i\omega}{h} Z_t(\omega) u_1^n = (-1)^{\frac{n-1}{2}} \rho\omega_n^2 \frac{e_{26}}{c_{66}} \frac{8V(1+R)}{n^2\pi^2}, \quad (45)$$

where ω_n is the nth eigenfrequency of the associated homogeneous problem. We note that Tiersten's original derivation of the scalar equation for electrically forced vibrations had a small error and a correction was later made in [11]. However, we believe that [11] still has a sign error in its (48) where the minus sign should be a plus sign. This sign difference results in a minor difference between (50) of [11] and our (45), i.e., in the right-hand side of (45), our ω_n^2 takes the place of the $(2\omega^2 - \omega_n^2)$ factor in [11]. We also note that the driving voltage is denoted by V in [11], and is denoted by $2V$ in the present paper. Therefore, in the right-hand side of (45), we have an "8" and (50) of [11] has a "4."

In light of the acoustic impedance, (20) and (45) are valid for time-harmonic motions only. In the derivation of (20) and (45), the plate top and bottom have the same acoustic impedance, which is assumed to be small. In the case when the acoustic impedance is only present on one surface of the plate, its effect can also be described by (20) and (45) by dropping the factor of 2 in the impedance term. This is similar to the use of the scalar equations in [34], [35] for both convex-convex and plano-convex resonators. The acoustic impedance may also be a slowly varying function of x_1 and x_3 when the spatial derivatives of the small and slowly varying impedance are negligible. This is similar to the approximation of neglecting the dependence of the electric potential on x_1 and x_3 in (1) [32], and is also similar to the situation wherein the equations derived in [34], [35] for plates with constant thickness were also used approximately to study contoured resonators.

IV. Dispersion Curves

For comparison and verification, we examine the dispersion curves for waves propagating in an unelectroded plate along x_1 determined from (20). These are shown in Fig. 2(a) for the case when $Z_t = 0$ (solid lines) where we have introduced the following dimensionless wave number and frequency:

$$X = 2h\xi/\pi, \quad \Omega = \sqrt{\rho/c_{66}}\, 2h\omega/\pi. \quad (46)$$

For small $|X|$, the solid lines are approximations of the odd TSh branches of the exact dispersion curves [45] with approximately the same intercepts on the frequency axis, the same slope when $X = 0$, and the same curvature when $X = 0$. Therefore (20) can be used to describe these waves approximately for small $|X|$ or long waves. When there are mass layers of thickness $2\bar{h}$ and density $\bar{\rho}$ on the surfaces of an unelectroded plate. It can be easily found that the surface acoustic impedance is

$$Z_t(\omega) = i\omega 2\bar{\rho}\bar{h}. \quad (47)$$

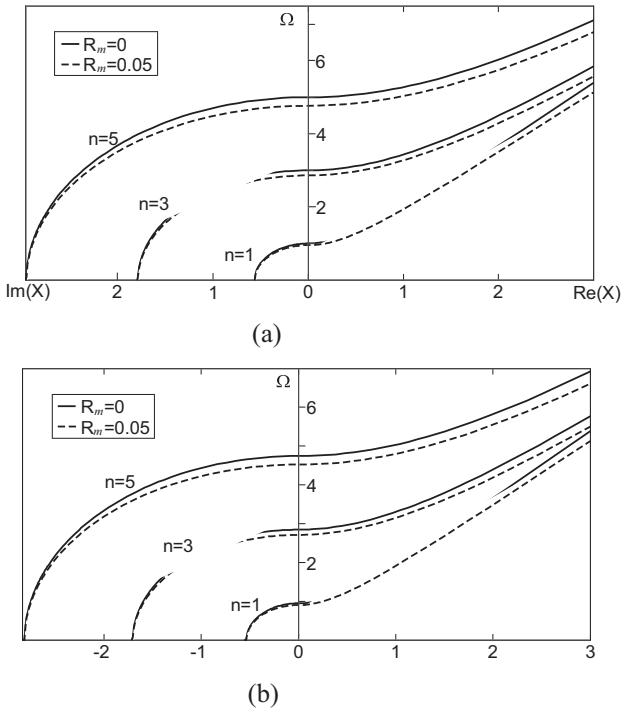

Fig. 2. (a) Dispersion curves determined by (20). Solid lines: $Z_t = 0$. Dotted lines: $R_m = 0.05$. (b) Dispersion curves determined by (34). Solid lines: $Z_t = 0$ and $R = 0.05$. Dotted lines: $R_m = 0.05$ and $R = 0.05$.

We denote the mass ratio by $R_m = 2\bar{\rho}\bar{h}/(\rho h)$. Dispersion curves for the case of $R_m = 0.05$ are shown by the dotted lines in Fig. 2(a). The dispersion curves become lower due to the inertia of the mass layers [46].

Similarly, for an electroded plate, the dispersion curves determined by (34) are shown in Fig. 2(b). The curves in Fig. 2(b) are systematically lower than those in Fig. 2(a) due to the electrode inertia.

When the plate is in contact with a fluid, the dispersion curves become complex reflecting a transition to damped waves due to the viscosity of the fluid [47].

V. Thickness Vibration of Unbounded Plates

In this section we compare the predictions by (20) and (34) with the results of the exact equations of piezoelectricity in the special case of pure TSh modes whose exact solutions can be obtained. For pure thickness modes in unbounded plates without x_1 and x_3 dependence, (20) leads to the following frequency equation for unelectroded plates:

$$\rho\omega^2 = \bar{c}_{66} \left(\frac{n\pi}{2h}\right)^2 + \frac{2i\omega}{h} Z_t(\omega). \quad (48)$$

For electroded plates (34) determines a frequency equation similar to (48), with $\bar{c}_{66}$ replaced by $\hat{c}_{66}$. In sensor applications, the first term on the right-hand side of (48) determines the unperturbed frequency denoted by ω_0 when $Z_t = 0$. In the case of small impedance which causes small frequency perturbations, the unknown frequency ω in the second term (which is small) on the right-hand side of (48) can be replaced by the known unperturbed frequency ω_0. Then (48) gives the

following approximate frequency perturbation:

$$\frac{\omega-\omega_0}{\omega_0}\cong\frac{4hi\omega_0}{n^2\pi^2\bar{c}_{66}}Z_t\left(\omega_0\right). \tag{49}$$

From the equations of linear piezoelectricity, pure thickness modes of an unelectroded AT-cut quartz plate are governed by the following differential equations and boundary conditions:

$$\begin{aligned}&c_{66}u_{1,22}+e_{26}\phi_{,22}=\rho\ddot{u}_1,\\&e_{26}u_{1,22}-\kappa_{22}\phi_{,22}=0,\end{aligned} \tag{50}$$

$$\begin{aligned}&T_{21}=-Z_t(\omega)\dot{u}_1,\quad D_2=0,\quad x_2=h,\\&T_{21}=Z_t\omega)\dot{u}_1,\quad D_2=0,\quad x_2=-h.\end{aligned} \tag{51}$$

For time-harmonic motions, (50) and (51) are ordinary differential equations with constant coefficients and can be solved in a standard procedure [10], [11]. They lead to the following frequency equation:

$$\tan\left(\eta h\right)=\bar{c}_{66}\eta h/[Z_t\left(\omega\right)i\omega h], \tag{52}$$

where $\eta=(\rho\omega^2/\bar{c}_{66})^{1/2}$.

For small impedance, by the same approximate procedure as the one used in obtaining (48), it can be obtained from (52) that

$$\omega\cong\sqrt{\frac{\bar{c}_{66}}{\rho}}\frac{n\pi}{2h}\left(1+\frac{4hi\omega}{n^2\pi^2\bar{c}_{66}}Z_t\left(\omega\right)\right), \tag{53}$$

which is the same as (49) for small Z_t.

Similarly, for electroded plates, it can also be shown that (34) and the corresponding frequency equation from the exact equations of piezoelectricity are approximately the same for small impedance. The result is

$$\omega=\sqrt{\frac{\bar{c}_{66}}{\rho}}\frac{n\pi}{2h}\left(1-R-\frac{4k_{26}^2}{n^2\pi^2}+\frac{4hi\omega}{n^2\pi^2\bar{c}_{66}}Z_t\left(\omega\right)\right). \tag{54}$$

As a specific example, consider a mass layer of thickness $2\bar{h}$ and density $\bar{\rho}$ on the top surface of an unelectroded plate. The surface acoustic impedance is given by (47). Substitution of (47) into (49), for one mass layer, (49) yields

$$\frac{\omega-\omega_0}{\omega_0}\cong-\frac{\bar{\rho}\,\bar{h}}{\rho\,h}, \tag{55}$$

which is the classical result for QCMs given in [1].

As another example, consider a semi-infinite fluid of density ρ_l and viscosity μ on the top of the crystal plate. In this case the impedance is

$$Z_t\left(\omega\right)=(1+i)\sqrt{\mu\rho_l\omega/2}. \tag{56}$$

Substitution of (56) into (49) yields

$$\frac{\omega-\omega_0}{\omega_0}\cong-\frac{\sqrt{2}\,(1-i)\,h\sqrt{\mu\rho_l}}{\bar{c}_{66}n^2\pi^2}\omega_0^{3/2}, \tag{57}$$

which is the classical result for fluid sensors in [12].

VI. Vibration of Rectangular Plates

More than being able to predict the frequencies of pure TSh modes, the main advantage of (20) and (34) is that they can describe the x_1 and x_3 dependence and therefore can be used to analyze finite plates. As an example, consider an unelectroded rectangular plate as shown in Fig. 1. The traction-free edge conditions are [35]

$$T_{12}\left(x_1=\pm a\right)=0,\quad T_{13}\left(x_3=\pm c\right)=0. \tag{58}$$

By the standard method of separation of variables, in a procedure similar to that in [35], from (20) we find:

$$u_1=A_{nml}\cos\left(l\pi\,x_3/c\right)\cos\left((2m+1)\,\pi\,x_1/(2a)\right), \tag{59}$$

$$\begin{aligned}\rho\omega^2=&\,c_{55}\left(\frac{l\pi}{c}\right)^2+M_n\left(\frac{(2m+1)\,\pi}{2a}\right)^2\\&+\bar{c}_{66}\left(\frac{n\pi}{2h}\right)^2+\frac{2i\omega}{h}Z_t\left(\omega\right).\end{aligned} \tag{60}$$

For electroded plates $\bar{c}_{66}$ is replaced by $\hat{c}_{66}$. (60) shows the dependence of frequency on the in-plane dimensions a and c. When the acoustic impedance is set to zero, (60) reduces to the result of [35].

VII. Conclusion

A single scalar differential equation is obtained for transversely varying TSh vibrations of rotated Y-cut quartz plates with surface impedance. The equation is accurate up to the second order of the in-plane wave numbers and generalizes some well-known equations in the literature. Both electroded and unelectroded plates are considered. The scalar differential equation can be used to analyze various finite quartz crystal microbalances for mass and liquid sensing.

References

[1] G. Sauerbrey, "Verwendung von schwingquarzen zur wägung dünner schichten und zur mikrowägung," *Zeitschrift Phys.*, vol. 155, no. 2, pp. 206–222, 1959.

[2] R. D. Mindlin, "High frequency vibrations of plated, crystal plates," in *Progress in Applied Mechanics* (The Prager Anniversary Volume), New York, NY, USA: Macmillan, 1963, pp. 73–84.

[3] J. L. Bleustein and H. F. Tiersten, "Forced thickness-shear vibrations of discontinuously plated piezoelectric plates," *J. Acoust. Soc. Amer.*, vol. 43, no. 6, pp. 1311–1318, 1968.

[4] J. A. Kosinski, "Thickness vibration of flat piezoelectric plates with massy electrodes of unequal thickness," in *Proc. IEEE Ultrason. Symp.*, Oct. 2003, pp. 70–73.

[5] J. G. Miller and D. J. Bolef, "Acoustic wave analysis of the operation of quartz-crystal film-thickness monitors," *J. Appl. Phys.*, vol. 39, no. 12, pp. 5815–5816, 1968.

[6] F. Boersma and E. C. van Ballegooyen, "Rotated Y-cut quartz crystal with two different electrodes treated as a one-dimensional acoustic composite resonator," *J. Acoust. Soc. Amer.*, vol. 62, no. 2, pp. 335–340, 1977.

[7] J. S. Yang, H. G. Zhou, and W. P. Zhang, "Thickness-shear vibration of rotated Y-cut quartz plates with relatively thick electrodes of unequal thickness," *IEEE Trans. Ultrason., Ferroelectr., Freq. Control*, vol. 52, no. 5, pp. 918–922, May 2005.

[8] E. Benes, M. Gröschl, W. Burger, and M. Schmid, "Sensors based on piezoelectric resonators," *Sens. Actuators A, Phys.*, vol. 48, no. 1, pp. 1–21, 1995.

[9] I. Koga, "Thickness vibrations of piezoelectric oscillating crystals," *Physics*, vol. 3, no. 2, pp. 70–80, 1932.

[10] H. F. Tiersten, "Thickness vibrations of piezoelectric plates," *J. Acoust. Soc. Amer.*, vol. 35, no. 1, pp. 53–58, 1963.

[11] H. F. Tiersten, "A corrected modal representation of thickness vibrations in quartz plates and its influence on the transversely varying case," *IEEE Trans. Ultrason., Ferroelectr., Freq. Control*, vol. 50, no. 11, pp. 1436–1443, Nov. 2003.
[12] K. K. Kanazawa and J. G. Gordon, "The oscillation frequency of a quartz resonator in contact with a liquid," *Anal. Chem. Acta*, vol. 175, no. 1, pp. 99–105, 1985.
[13] C. E. Reed, K. K. Kanazawa, and J. H. Kaufman, "Physical description of a viscoelastically loaded AT-cut quartz resonator," *J. Acoust. Soc. Amer.*, vol. 68, no. 5, pp. 1993–2001, 1990.
[14] S. J. Martin, V. E. Granstaff, and G. C. Frye, "Characterization of a quartz crystal microbalance with simultaneous mass and liquid loading," *Anal. Chem.*, vol. 63, no. 20, pp. 2272–2281, 1991.
[15] W. C. Duncan-Hewitt and M. Thompson, "Four-layer theory for the acoustic shear wave sensor in liquids incorporating interface slip and liquid structure," *Anal. Chem.*, vol. 64, no. 1, pp. 94–105, 1992.
[16] F. Ferrante, A. L. Kipling, and M. Thompson, "Molecular slip at the solid-liquid interface of an acoustic-wave sensor," *J. Appl. Phys.*, vol. 76, no. 6, pp. 3448–3462, 1994.
[17] J. Wang and L. J. Shen, "Exact thickness-shear resonance frequency of electroded piezoelectric crystal plates," *J. Zhejiang Univ. Sci. A*, vol. 6, no. 9, pp. 980–985, 2005.
[18] J. S. Yang, Y. T. Hu, Y. Zeng, and H. Fan, "Thickness-shear vibration of rotated Y-cut quartz plates with imperfectly bounded surface mass layers," *IEEE Trans. Ultrason., Ferroelectr., Freq. Control*, vol. 53, no. 1, pp. 241–245, Jan. 2006.
[19] Y. Jing, J. Chen, X. Chen, and X. Gong, "Frequency shift of thickness-shear vibrations of AT-cut quartz resonators due to a liquid layer with the electrode stiffness considered," *IEEE Trans. Ultrason., Ferroelectr., Freq. Control*, vol. 54, no. 7, pp. 1290–1292, Jul. 2007.
[20] B. Liu, Q. Jiang, and J. S. Yang, "Fluid-induced frequency shift in a piezoelectric plate driven by lateral electric fields," *Int. J. Appl. Electromag. Mech.*, vol. 34, no. 3, pp. 171–180, 2010.
[21] B. Liu, Q. Jiang, and J. S. Yang, "Frequency shifts in a quartz plate piezoelectric resonator in contact with a viscous fluid under a separated electrode," *Int. J. Appl. Electromag. Mech.*, vol. 35, no. 3, pp. 177–187, 2011.
[22] J. R. Vig and A. Ballato, "Comments on the effects of nonuniform mass loading on a quartz crystal microbalance," *IEEE Trans. Ultrason., Ferroelectr., Freq. Control*, vol. 45, no. 5, pp. 1123–1124, Sep. 1998.
[23] V. E. Bottom, *Introduction to Quartz Crystal Unit Design*. New York, NY, USA: Van Nostrand Reinhold, 1982.
[24] F. Shen, K. H. Lee, S. J. O'Shea, P. Lu, and T. Y. Ng, "Frequency interference between two quartz crystal microbalances," *IEEE Sensors J.*, vol. 3, no. 3, pp. 274–281, Jun. 2003.
[25] F. Shen and P. Lu, "Influence of interchannel spacing on the dynamical properties of multichannel quartz crystal microbalance," *IEEE Trans. Ultrason., Ferroelectr., Freq. Control.*, vol. 51, no. 2, pp. 249–253, Feb. 2004.
[26] N. Liu, J. S. Yang, and J. Wang, "Analysis of a monolithic, two-dimensional array of quartz crystal microbalances loaded by mass layers with nonuniform thickness," *IEEE Trans. Ultrason., Ferroelectr., Freq. Control*, vol. 59, no. 4, pp. 746–751, Apr. 2012.
[27] B. A. Martin and H. E. Hager, "Velocity profile on quartz crystals oscillating in liquids," *J. Appl. Phys.*, vol. 65, no. 7, pp. 2630–2635, 1989.
[28] P. J. Cumpson and M. P. Seah, "The quartz crystal microbalances; radial/polar dependence of mass sensitivity both on and off the electrodes," *Meas. Sci. Technol.*, vol. 1, no. 7, pp. 544–555, 1990.
[29] F. Josse and Y. Lee, "Analysis of the radial dependence of mass sensitivity of modified electrode quartz crystal resonators," *Anal. Chem.*, vol. 70, no. 2, pp. 237–247, 1998.
[30] N. Liu, J. S. Yang, and W. Q. Chen, "Effects of mass layer nonuniformity on a quartz crystal microbalance," *IEEE Sensors J.*, vol. 11, no. 4, pp. 934–938, Apr. 2011.
[31] N. Liu, J. S. Yang, and W. Q. Chen, "Effects of a mass layer with gradually varying thickness on a quartz crystal microbalance," *IEEE Sensors J.*, vol. 11, no. 8, pp. 1635–1639, Aug. 2011.
[32] H. F. Tiersten, "Analysis of intermodulation in thickness-shear and trapped energy resonators," *J. Acoust. Soc. Amer.*, vol. 57, no. 3, pp. 667–681, 1975.
[33] H. F. Tiersten, "Analysis of trapped-energy resonators operating in overtones of coupled thickness-shear and thickness-twist," *J. Acoust. Soc. Amer.*, vol. 59, no. 4, pp. 879–888, 1976.
[34] H. F. Tiersten and R. C. Smythe, "An analysis of contoured crystal resonators operating in overtones of coupled thickness shear and thickness twist," *J. Acoust. Soc. Amer.*, vol. 65, no. 6, pp. 1455–1460, 1979.
[35] H. F. Tiersten and R. C. Smythe, "Coupled thickness-shear and thickness-twist vibrations of unelectroded AT-cut quartz plates," *J. Acoust. Soc. Amer.*, vol. 78, no. 5, pp. 1684–1689, 1985.
[36] B. K. Sinha and D. S. Stevens, "Thickness-shear vibrations of a beveled AT-cut quartz plate," *J. Acoust. Soc. Amer.*, vol. 66, no. 1, pp. 192–196, 1979.
[37] A. V. Apostolov and S. H. Slavov, "Frequency spectrum and modes of vibration in circular, convex AT-cut bevelled-design quartz resonators," *Appl. Phys. A, Mater. Sci. Process*, vol. 29, no. 1, pp. 33–37, 1982.
[38] S. Hertl, L. Wimmer, and E. Benes, "Investigation of the amplitude distribution of AT-cut crystals," *J. Acoust. Soc. Amer.*, vol. 78, no. 4, pp. 1337–1343, 1985.
[39] S. H. Slavov, "Modes of vibration, motion inductance, and resonance interval of circular, convex AT-cut beveled design trapped energy quartz resonators," *Appl. Phy. A, Mater. Sci. Process*, vol. 40, no. 1, pp. 59–65, 1986.
[40] E. P. EerNisse, L. D. Clayton, and M. H. Watts, "Distortions of thickness shear mode shapes in plano-convex quartz resonators with mass perturbation," *IEEE Trans. Ultrason., Ferroelectr., Freq. Control*, vol. 37, no. 6, pp. 571–576, Nov. 1990.
[41] P. Li, F. Jin, and J. S. Yang, "Thickness-shear vibration of an AT-cut quartz resonator with a hyperbolic contour," *IEEE Trans. Ultrason., Ferroelectr., Freq. Control*, vol. 59, no. 5, pp. 1006–1012, May 2012.
[42] A. Ballato, "Piezoelectric resonators loaded with viscoelastic and nonuniform media," in *Proc. IEEE Int. Freq. Control Symp. PDA Exhibit.*, May 2002, pp. 191–201.
[43] T. Voglhuber-Brunnmaier and B. Jacoby, "Efficient spectral domain formulation of loading effects in acoustic sensors," *Sens. Actuators A, Phys.*, vol. 186, pp. 38–47, Oct. 2012.
[44] Y. Y. Chen, J. Wang, J. K. Du, W. P. Zhang, and J. S. Yang, "Effects of air resistance on AT-cut quartz thickness-shear resonators," *IEEE Trans. Ultrason., Ferroelectr., Freq. Control*, vol. 60, no. 2, pp. 402–407, Feb. 2013.
[45] J. Wang, L. J. Yang, and J. K. Du, "The dispersion relations and vibration modes of infinite quartz crystal plates at higher frequencies," in *Proc. Joint Conf. Symp. Piezoelectr., Acoustic Waves Device Appl. China Symp. Freq. Control Technol.*, 2009, pp. 494–499.
[46] L. Yang, J. K. Du, J. Wang, and J. S. Yang, "Shear-horizontal waves in a rotated Y-cut quartz plate with an isotropic elastic layer of finite thickness," *Acta Mech. Solida Sinica*, vol. 25, no. 1, pp. 82–89, 2012.
[47] J. B. Sun, J. K. Du, J. S. Yang, and J. Wang, "Shear-horizontal waves in a rotated Y-cut quartz plate in contact with a viscous fluid," *Ultrasonics*, vol. 52, no. 1, pp. 133–137, 2012.

Huijing He, photograph and biography are not available at the time of publication.

Jiashi Yang, photograph and biography are not available at the time of publication.

John A. Kosinski, photograph and biography are not available at the time of publication.